An Enhanced Single-Phase Self-Tuning Filter based Open-Loop Frequency Estimator for Weak Grid

Verma, Anant Kumar; Ahmed, Hafiz; Roncero-Sánchez, Pedro ; Chaturvedi, Pradyumn

2021 IEEE Energy Conversion Congress and Exposition (ECCE)

An Enhanced Single-Phase Self-Tuning Filter based Open-Loop Frequency Estimator for Weak Grid

Anant Kumar Verma*, Hafiz Ahmed†, Pedro Roncero-Sánchez‡, and Pradyumn Chaturvedi††

*Electrical Engineering Department, National Institute of Technology Hamipur, H.P., India, 177005
†Nuclear Futures Institute, Bangor University, United Kingdom, LL57 1UT
‡Department of EECEC, Universidad de Castilla-La Mancha, Spain, 13071
††Visvesvaraya National Institute of Technology, Nagpur, Maharashtra, India, 440012
Email: *Anant_verma12@ieee.org, †Hafiz.h.ahmed@ieee.org,‡Pedro.roncero@uclm.es, ††Pc220774@gmail.com

Abstract—This article proposes an enhanced single-phase self-tuning pre-filter for estimating the fundamental grid voltage frequency. The known extended self-tuning filter (STF) adheres to an increased structural complexity, which may consume memory in the digital hardware to estimate the fundamental grid voltage signal. The proposed STF, which relies on a simple non-adaptive comb filter, may address this issue. Consequently, the introduction of imaginary zeros ensures better rejection of the DC-offset and the harmonic components while keeping the proposed filter structure simpler to implement. Furthermore, a simple open-loop frequency estimator is proposed, which does not involve any inverse trigonometric function to estimate the fundamental frequency. This entire proposal is cost-effective and has good frequency tracking abilities with a reduced computational load. The experimental results imply the suitability of the proposed scheme for weak inertia power grid networks where synthetic inertia controllers require a rapid frequency information to control the injected power under adverse grid voltage conditions.

Index Terms—Frequency estimation, moving average filter, orthogonal signal generation, self-tuning filter, single-phase grid

I. INTRODUCTION

The high penetration of distributed renewable energy sources (i.e., solar panels, wind turbines, etc.) into the power grid network through the use of static power conversion equipments may decrease the actual inertial component of the grid [1]. This indicates to optimally regulate the voltage and frequency parameters in the presence of grid-tied power converters (i.e., Inverters). Thus, the concept of synthetic inertia is introduced, which states that the control architecture of the grid-connected converter (GCC) must provide virtual inertia similar to a synchronous machine to maintain the grid stability. In the case of weak inertia grids, the control of GCC mainly relies on the accurate information of the fundamental grid voltage frequency [2]. For this purpose, several techniques are proposed in literature as follows: phase-locked loops (PLLs) [3], [4], frequency-locked loops (FLLs) [5] and open-loop schemes [6]. It is well known that PLLs and FLLs are dynamically slower owing to the closed-loop nature. In addition, the dynamic performance is severely affected by the choice of the filtering scheme and controller tuning methods.

On the other hand, open-loop frequency estimation schemes are free from tedious controller tuning process and are easily implementable on a real-time digital hardware. In single-phase applications, orthogonal signal generation (OSG) [7] approach is widely adopted to ease out the challenge for estimating three fundamental grid voltage parameters, i.e., amplitude, phase and frequency. The prevalent OSG approaches [7] are as follows: second order generalized integrator (SOGI), moving average filter based OSG, demodulation based OSG, transport delay approach, etc.

Interestingly, the discrete time implementation of any estimation algorithm is highly encouraged from the view point of hardware cost and memory utilization. However, the discrete time delay blocks may cause instability issues and yield additional poles which may result in higher order systems [8]. The effect of discretization on the stability of proportional resonant controller is studied in [9] and the study suggests the use of reliable discretization methods. Nevertheless, variable sampling methods [10] can be adopted so as to obtain grid frequency adaptability under off-nominal frequency deviations. However, the specially designed numerically controlled oscillator is still prone to double frequency component owing to the presence of DC-offset and harmonics in the grid signal. Note that synchronous sampling is not always preferred owing to the readily available fixed-frequency sampling based low cost embedded hardware. Thus, an efficient low sampling frequency based two-sample PLL technique is proposed in [11]. However, high sampling frequency may offer better accuracy in the estimation [12], but at the expense of an increase in hardware cost and memory storage. In this study, an enhanced version of well-known self-tuning filter [13] is designed optimally to provide better immunity towards DC-offset and harmonics. Importantly, the proposed enhanced SFT is computationally simpler to implement as compared to recently proposed extended STF [14]. In addition, a simple open-loop frequency estimator is proposed, when combined with the enhanced STF will provide better estimates of the fundamental frequency.

II. PROPOSED ENHANCED SELF-TUNING FILTER

In this section, a conventional self-tuning filter (CSTF) useful for three-phase application is modified to present its application in single-phase power systems. In general, the

CSTF requires orthogonal components (OCs) for its proper operation. Therefore, the Clarke's transformation is an useful tool for obtaining the orthogonal components (v_α, v_β) from a harmonically distorted three-phase grid voltage signal (v_{abc}), as shown in Fig. 1. Thereby, the application of CSTF can provide fundamental orthogonal signals (FOCs) which are beneficial for control of grid-tied converters. Moroever, the accurate extraction of an orthogonal component from a single-phase grid voltage signal is a tedious task. For this purpose, many OSG approaches were reported in literature [7]. Nevertheless, the improvement in the CSTF structure is essential for obtaining the FOCs in case of single-phase power systems. The transfer function of the CSTF is given below:

$$H(s) = \rho \frac{s + \rho + j\omega_o}{(s+\rho)^2 + \omega_o^2} \tag{1}$$

where $\omega_o = 2\pi/T_o$ ($T_o = 1/f_o$, $f_o = 50$ Hz) and $\rho = f_o$ are the cut-off frequency and fixed tuning gain, respectively. The structure of CSTF is presented in Fig. 1.
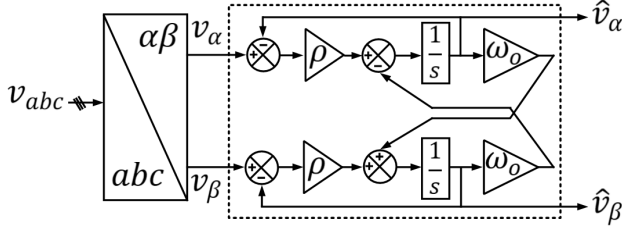

Fig. 1. Conventional single-phase self-tuning filter.

The parameter ρ was introduced to obtain a trade-off between the dynamic response time and harmonic rejection abilities while retaining an unity gain filter structure. The frequency domain input $(V_\alpha(s), V_\beta(s))$ and the output $(\hat{V}_\alpha(s), \hat{V}_\beta(s))$ relationships between the actual $(v_\alpha(t), v_\beta(t))$ and the FOCs $(\hat{v}_\alpha(t), \hat{v}_\beta(t))$ are expressed as follows:

$$\hat{V}_\alpha(s) = \frac{\rho}{s}[V_\alpha(s) - \hat{V}_\alpha(s)] - \frac{\omega_o}{s}\hat{V}_\beta(s) \tag{2}$$

$$\hat{V}_\beta(s) = \frac{\rho}{s}[V_\beta(s) - \hat{V}_\beta(s)] - \frac{\omega_o}{s}\hat{V}_\alpha(s) \tag{3}$$

Note that (2) and (3) still converges slowly to the desired states, i.e., $\hat{v}_\alpha(t)$ and $\hat{v}_\beta(t)$. Hence, the CSTF structure is modified using a comb filter, as exemplified in Fig. 1.
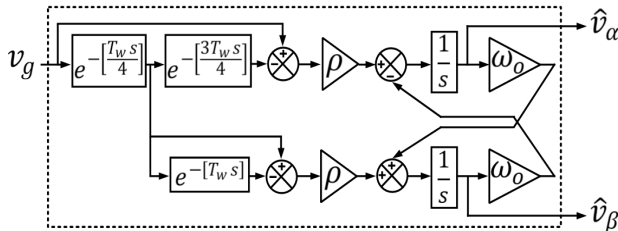

Fig. 2. Proposed single-phase self-tuning filter.

In the case of proposed STF, the frequency domain input (V_g) and the output $(\hat{V}_\alpha, \hat{V}_\beta)$ relationships between $v_g(t)$ and the FOCs are expressed as follows:

$$\hat{V}_g = \frac{\rho V_g(s)}{s}[1 - e^{-T_w s}] - \frac{\omega_o}{s}\hat{V}_\beta \tag{4}$$

$$\hat{V}_g = \frac{\rho V_g(s)e^{-\frac{T_w s}{4}}}{s}[1 - e^{-T_w s}] + \frac{\omega_o}{s}\hat{V}_\alpha \tag{5}$$

where $T_w = 2\pi/\omega_o$ is the window length. The harmonic and DC-offset rejection abilities of the proposed STF compared to the well-known CSTF [13] and the extended STF [14] are compared using frequency response analysis (see Fig. 3).
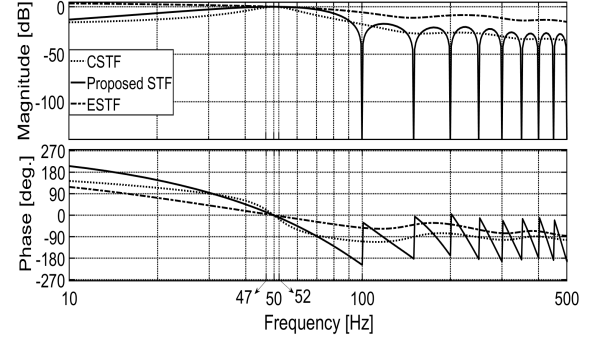

Fig. 3. Bode response plots of the proposed STF, CSTF and ESTF.

Note that the proposed STF has better DC-offset and harmonic rejection capability when compared to the CSTF and the ESTF. Hence, an improved STF can be developed as compared to the single-phase version of the CSTF applied for an active power filter (APF) application, reported in [13]. Further, the harmonic and the DC-offset free FOCs obtained in the output of proposed STF are denoted as follows:

$$\hat{v}_\alpha(t) = A\sin(\omega_1 t + \phi) \tag{6}$$

$$\hat{v}_\beta(t) = A\cos(\omega_1 t + \phi) \tag{7}$$

where $A = \sqrt{(\hat{v}_\alpha)^2 + (\hat{v}_\beta)^2}$ and ω_1 are the fundamental amplitude and the unknown angular grid frequency. In order to determine ω_1 and to solve control issues regarding the proper operation of grid-tied converters, the detection of fundamental phase, frequency and amplitude is highly desired. For this purpose, the PLL and/or open-loop frequency estimators with the combination of OSGs are very attractive. Hence, an open-loop frequency estimator is proposed in this work, which helps detecting the fundamental frequency information.

III. GRID FREQUENCY ESTIMATION ALGORITHM

In general, the PLL algorithms are often employed in the control structure of grid tied inverters for obtaining fundamental phase, amplitude and frequency information. However, the dynamic performance of the PLL is affected with the choice of tuning gain parameters. Therefore, an effortless tuning based computationally simple three-point angular frequency estimation technique, as proposed by J. Shekel [15], is employed in this work. Note that the proposal suggested in [15] suffers from a numerically-ill condition owing to the

mathematical operations applied to the fundamental sinusoidal component. Hence, a simple modification helps eliminating the ill-condition. In order to generalize the concept, it can be stated that for a given curve $f(t)$, a sinusoidal curve expressed as $A\,sin(\omega t + \phi)$ may be fitted to any three consecutive points. For further clarification, let us assume, $Q = Q(t) = A \sin(\omega t + \phi)$. Note that $Q(t)$ must be single valued, continuous, and twice differentiabe [15]. Thus, the points which passes through $Q(t)$ are defined as follows:

$$Q_1 = Q(t + \Delta t) = A \sin(\omega_1 t + \phi + \omega_1 \Delta t) \quad (8)$$

$$Q_2 = Q(t - \Delta t) = A \sin(\omega_1 t + \phi - \omega_1 \Delta t) \quad (9)$$

From (8) and (9), a general solution can be deduced as follows:

$$\tan(\omega_1 \Delta t) = \frac{\sqrt{(2Q + Q_1 + Q_2)(2Q - Q_1 - Q_2)}}{Q_1 + Q_2} \quad (10)$$

The transcendental equation (10) is solved using approximation considered in [15] which yields the estimated frequency as follows: $\hat{\omega}_1 = \sqrt{\frac{-\ddot{Q}}{Q}}$, where, $\ddot{Q}$ is the second derivative of function $Q(t)$. However, $\hat{\omega}_1$ suffers from a numerically ill-condition whenever $Q(t) = 0$, resulting in an erroneous estimate of frequency. This situation can be avoided by considering the FOCs. It is simple to understand that the FOCs are, therefore, differentiated twice as follows:

$$\ddot{v}_\alpha(t) = -\omega_1^2 A\,sin(\omega_1 t + \phi) \quad (11)$$

$$\ddot{v}_\beta(t) = -\omega_1^2 A\,cos(\omega_1 t + \phi) \quad (12)$$

Squaring and adding, (11) and (12) results in,

$$(\ddot{v}_\alpha(t))^2 + (\ddot{v}_\beta(t))^2 - \omega_1^4 A^2 = 0 \quad (13)$$

From (13), a first order discrete time model can be obtained to determine ω_1, given below:

$$P(n) = r(n)Q(n) \quad (14)$$

where $Q = A^2$, $r = \omega^4$, $P = (\ddot{v}_\alpha)^2 + (\ddot{v}_\beta)^2$ and n is the discrete time sampling instant. The parameter $r(n)$ can be obtained by minimizing the function given below:

$$J(n) = \frac{1}{2}\sum_{k=0}^{n} \gamma^{n-k}[P(k) - r(n)Q(k)]^2 \quad (15)$$

where γ is known as forgetting factor lies in the range of $[0, 1)$. A low value of γ helps to control the convergence rate of the algorithm with improvement in the harmonic rejection ability. On the other hand, larger value of γ affects the overshoot in the fundamental frequency and the harmonic rejection capability. The value of $r(n)$ can be obtained by differentiating (15) and equating it to zero as follows:

$$r(n) = \frac{\sum_{k=0}^{n} \gamma^{n-k}[P(k)Q(k)]}{\sum_{k=0}^{n} \gamma^{n-k}[Q(k)]^2} \quad (16)$$

Using (16), $r(n)$ can be recursively obtained as follows:

$$r(n) = \frac{\gamma\zeta(n-1)r(n-1) + P(k)Q(k)}{\zeta(n)}, \quad (17)$$

$$\zeta(n) = \sum_{k=0}^{n} \gamma^{n-k}[Q(k)]^2 = \gamma\zeta(n-1) + [Q(k)]^2$$

The estimated frequency is,

$$\hat{f}_1 = \frac{\sqrt[4]{r(n)}}{2\pi} \quad (18)$$

Note that the estimated frequency can be computed without a numerically ill-condition as shown in Fig. 4. Hence,
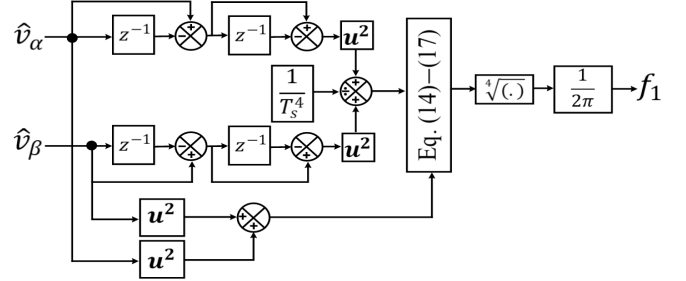

Fig. 4. Proposed fundamental frequency estimator

this provides an opportunity to use the real-time embedded hardware platform in an optimal way without increasing the computational load. However, a low-pass filter i.e., half-cycle moving average filter (MAF) [3], is still required to attenuate the steady-state ripples in the estimate of frequency under off-nominal conditions. Note that the errors in the fundamental
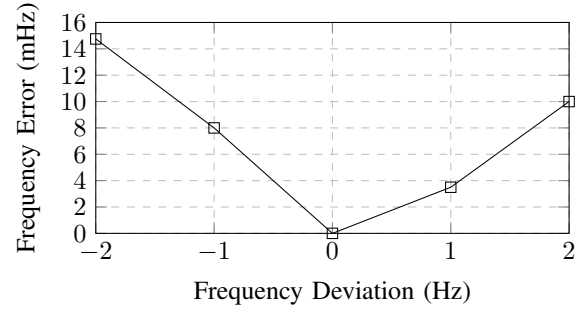

Fig. 5. Errors in the estimated frequency when the supply voltage is harmonically distorted.

frequency other than the nominal frequency are below 15 mHz which is a maximum permissible limit specified by the IEC 61000-4-7 standard.

IV. SIMULATION RESULTS

The simulation study is performed in MATLAB/Simulink environment at a sampling frequency of 10kHz. Further, the simulations results are divided into two categories i.e. 1) To perform comparative performance evaluation with the known frequency estimation algorithms and 2) To analyze the performance of the proposed OSG when applied to a single-phase APF application. The grid voltage parameters are 1 p.u. at 50 Hz with a total harmonic distortion (THD) of 10.67% while the harmonics, i.e., $h = $ 3, 5, 7, 9, 11, 13, 15, 17 are considered as per EN 50160 standard [16]. The proposed scheme is compared with the single-phase configuration of CSTF-PLL [13] and ESTF-PLL [14] techniques along with a

demodulation based PLL [4]. The control parameters for DT-PLL are $\alpha = 400$, $\beta = 50$ and $\gamma = 50$. The tuning parameter $\rho = 50, 150$ is chosen for the CSTF-PLL and the ESTF-PLL, respectively. Similarly, the parameters for the proposed scheme are $\rho = 50$ and $\gamma = 0.96$.

A. Comparative performance evaluation

The proposed scheme and the DT-PLL are found immune to the presence of DC-offset component in the grid voltage signal, as shown in Fig. 6. However, DT-PLL suffers from a 0.5 Hz overshoot in the estimate of frequency. In addition, the ESTF-PLL and CSTF-PLL are incapable to handle the DC-offset component present in the grid signal. Further, the
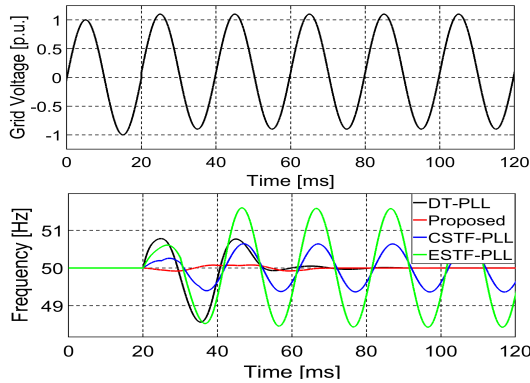

Fig. 6. Estimation of frequency in the presence of 10% of DC-offset.

harmonic rejection ability at nominal frequency i.e. 50 Hz is presented in Fig. 7. Note that the proposed scheme, ESTF-PLL and CSTF-PLL has good harmonic rejection ability when compared to the DT-PLL. Moreover, the proposed scheme can settle to a next steady-state within 2.5 times of a fundamental cycle. On the other hand, the ESTF-PLL, the DT PLL and
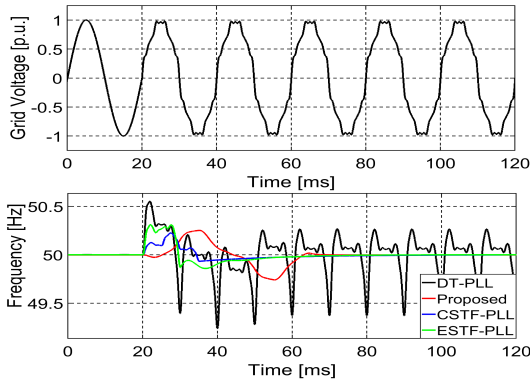

Fig. 7. Estimation of frequency in the presence of harmonics.

the proposed scheme adheres to a comparable overshoot in the estimate of frequency when grid voltage suffers from a 30° phase jump, as depicted in Fig. 8. Nevertheless, the proposed frequency estimator and the DT-PLL can settle to a next steady-state faster as compared to the ESTF-PLL and CSTF-PLL. Further, the ability to handle the voltage sag in the grid voltage signal is shown in Fig. 9.
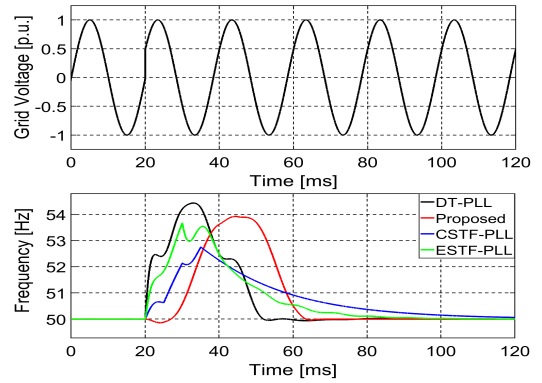

Fig. 8. Estimation of frequency in the presence of 30° phase jump.
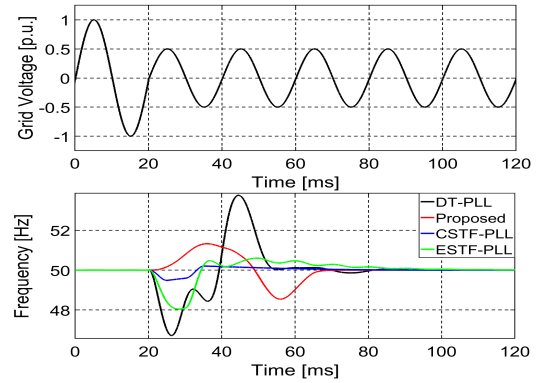

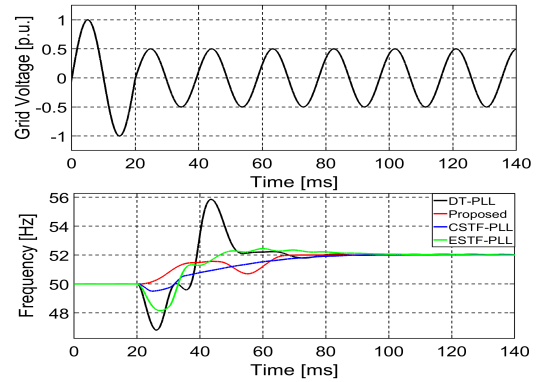Fig. 9. Estimation of frequency in the presence of 50% voltage sag.

Fig. 10. Frequency step tracking in the presence of 50% voltage sag.

Note that the DT-PLL is sensitive to the voltage sag as compared to the other schemes. Nevertheless, the proposed algorithm has fast frequency tracking ability as compared to all other schemes. Similarly, a frequency step tracking ability is shown in Fig. 10, when 50% voltage sag is considered in the grid voltage signal. It can be observed that the proposed frequency estimator and the CSTF-PLL does not suffer from overshoot in the estimate of frequency. However, the DT-PLL and the ESTF-PLL suffers from 4 Hz and 0.4 Hz of overshoot in the estimate of frequency, respectively. In Fig. 11, the off-nominal harmonic rejection capability is presented. The proposed frequency estimator is able to track the frequency
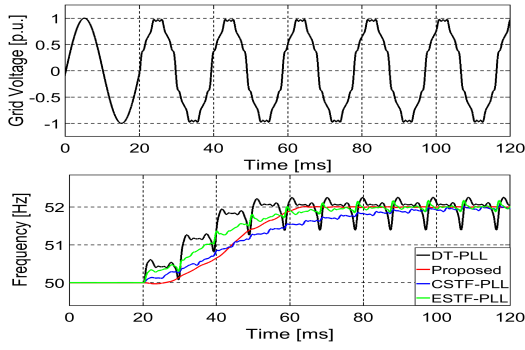
Fig. 11. Frequency step tracking in the presence of harmonics.

within two fundamental cycles with a negligible amount of error in the estimate of frequency. The performance of ESTF-PLL and the DT-PLL are severely affected in the presence of harmonics under-off-nominal frequency conditions. Moreover, the CSTF-PLL is dynamically slower in response. Hence, the proposed solution may be a suitable choice for single-phase weak grids and active power filter applications.

B. Proposed STF based single-phase active power filter

In general, improving the power quality of the utility grid is a challenging task. Hence, the APFs can help improving the power quality of the grid. A good control over APF usually achieved with the employment of STF in the control structure of a generic single-phase APF, as shown in Fig. 12. Therefore, the proposed STF is implemented in the control structure of the generic single-phase APF application as provided in [13]. The extraction of the fundamental component from
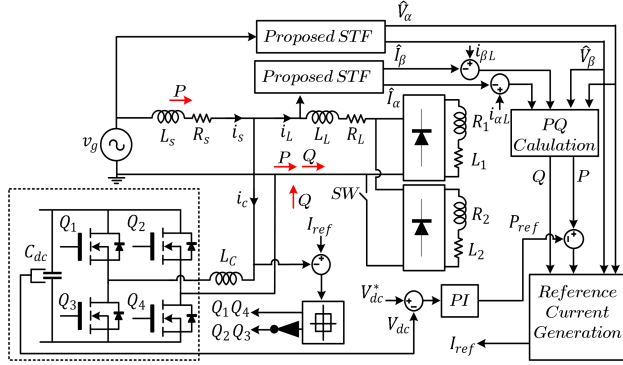

Fig. 12. Generic single-phase active power filter configuration.

the non-linear load current (i_L) component (i.e., $\hat{I}_{\alpha L}$, $\hat{I}_{\beta L}$) and the fundamental component from the grid voltage signal (v_g) helps in generating accurate reference current (I_{ref}). Thereby, a good control over inverter and the DC-Link voltage (V_{dc}) can be achieved while injection of required amount of compensating current (i_c) can easily takes place. This process helps in reducing overall THD in the source current (i_s) while complying with the IEEE-519 standard [13]. In the absence of the proposed STF, the THD in $i_s = i_L$ is $\approx 26\%$ and grid voltage is distorted as per EN50160 standard. When the non-linear loads i.e. $R_1 = 30\ \Omega$ and $L_1 = 80$mH and $R_1 = 40\ \Omega$ and $L_1 = 80$ mH along with the parameters $L_s = 1\ \mu$H,
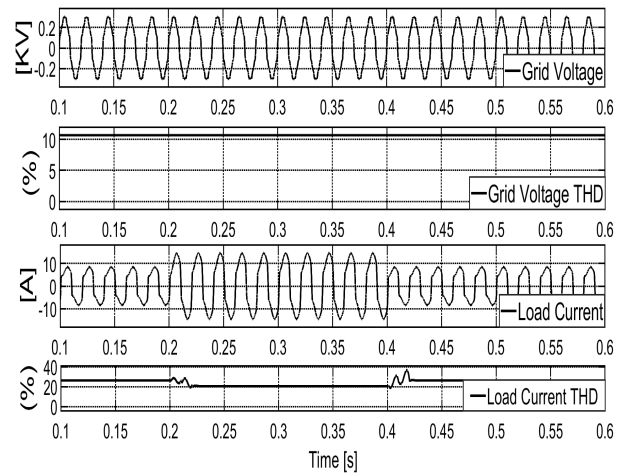

Fig. 13. Harmonically distorted supply voltage with non-linear load current.
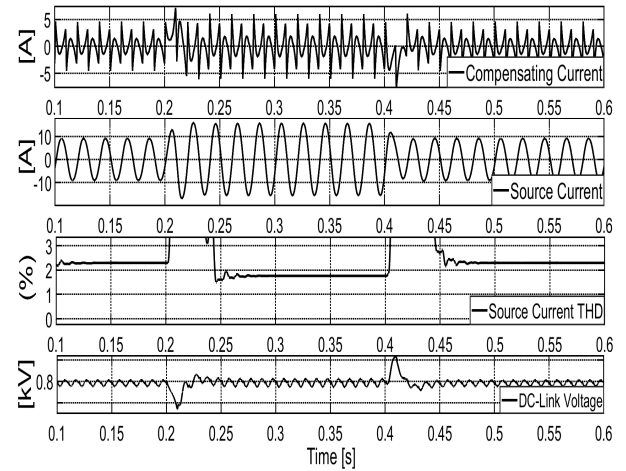

Fig. 14. Dynamics of compensating current, source current and DC-link voltage.

$L_L = 8$mH and $L_c = 20$mH, as shown in Fig. 13, the i_s behaves as non-linear current which is responsible for the power quality degradation. On the other hand, the involvement of proposed STF based APF whose V_{dc} is maintained at 800 V using a PI controller and C_{dc} (2000μF), helps to reduce the THD well below 3% by properly injecting the i_c in the utility grid. Moreover, the variations in the load does not severely affect the dynamics of the DC-link voltage while fast injection of the compensating current can be maintained within two times of the fundamental cycle, (see Fig. 14).

V. EXPERIMENTAL EVALUATION

The real time validation of the proposed frequency estimator is carried out using dSPACE DS1104 controller. A fixed step solver with a sampling frequency of 10 kHz is considered. The automatic code generation approach is utilized for uploading the complied code to DS1104 controller. The grid voltage signal is then supplied to the algorithms under evaluation for three different test conditions. The results are captured on an oscilloscope from digital-to-analog converters of the in-put/output board. In Fig. 15, 50% voltage sag, 30° phase jump

and 10% of DC-offset in the grid voltage signal is supplied to all the schemes. It can be observed that the proposed frequency
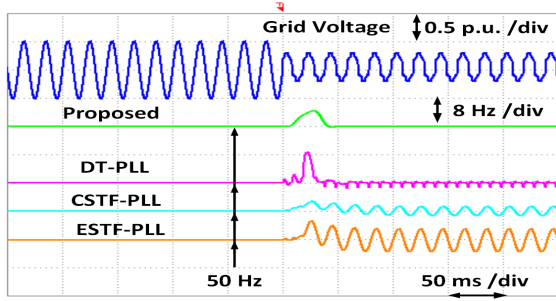

Fig. 15. Combined voltage sag, phase jump and DC-offset at nominal frequency condition.

estimation scheme has better DC-offset and harmonic rejection ability as compared to other schemes. In addition, the DT-PLL and the proposed estimator suffer from an overshoot in the estimate of frequency i.e. 8 Hz and 4 Hz, respectively. Similarly, in case of frequency ramp (Fig. 16) and frequency step (Fig. 17), the proposed frequency estimation algorithm has a better dynamic performance. Moreover, a better steady-
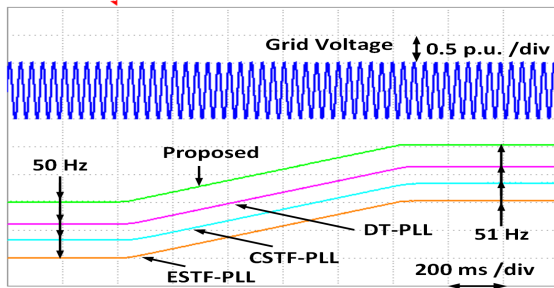

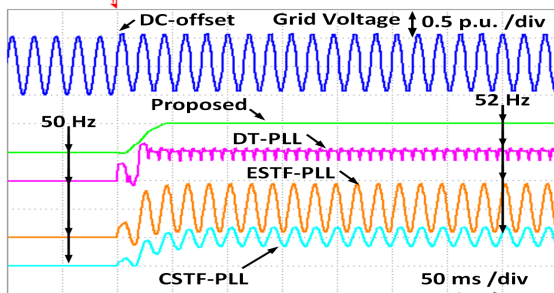Fig. 16. Frequency ramp tracking performance i.e. 50-51 Hz

Fig. 17. Frequency step from 50 Hz to 52 Hz in the presence of harmonics and 10% of DC-offset.

state accuracy is achieved within two times of the fundamental cycle. Hence, the proposed STF based frequency estimator is a useful approach for detection of fundamental frequency in single-phase applications.

VI. Conclusion

An improved and computationally less demanding self-tuning filter based open-loop frequency estimation technique is proposed for single-phase weak inertia grids. With the inclusion of a comb filter, the conventional STF can be effectively employed for single-phase application with good immunity towards DC-offset and harmonics. To better utilize the memory allocated in any embedded hardware, a simple open-loop frequency estimator is proposed which could be easily employed at lower sampling frequencies. In addition, experimental results confirm the better dynamic tracking ability of the proposed scheme for providing frequency support.

References

[1] F. Wilches-Bernal, J. Wold, and W. H. Balliet, "A method for correcting frequency estimates for synthetic inertia control," IEEE Access, vol. 8, pp. 229141–229151, Dec. 2020.
[2] G. Liu, J. Zhu, H. Zhou, W. Wang, and W. Wang, "A novel FLL for single-phase grid-connected PV inverter under weak grid," in IECON Conf. of the IEEE Indus. Electron. Soc., Oct. 2020, pp. 3353–3358.
[3] S. Golestan, J. M. Guerrero, and J. C. Vasquez, "Single-phase PLLs: A review of recent advances," IEEE Trans. on Power Electron., vol. 32, no. 12, pp. 9013–9030, Dec. 2017.
[4] H. Ahmed and M. Benbouzid, "Demodulation type single-phase PLL with DC offset rejection," IET Electron. Letters, vol. 56, no. 7, pp. 344–347, Apr. 2020.
[5] H. Ahmed, S. Amamra, and M. Bierhoff, "Frequency-locked loop-based estimation of single-phase grid voltage parameters," IEEE Trans. on Indus. Electron., vol. 66, no. 11, pp. 8856–8859, Nov. 2019.
[6] A. Safa, E. M. Berkouk, Y. Messlem, Z. Chedjara, and A. Gouichiche, "A pseudo open loop synchronization technique for heavily distorted grid voltage," Elec. Power Sys. Res., vol. 158, pp. 136–146, 2018.
[7] Y. Han, M. Luo, X. Zhao, J. M. Guerrero, and L. Xu, "Comparative performance evaluation of orthogonal-signal-generators-based single-phase PLL algorithms-A survey," IEEE Trans. on Power Electron., vol. 31, no. 5, pp. 3932–3944, May 2016.
[8] J. Wilson, A. Nelson, and B. Farhang-Boroujeny, "Parameter derivation of type-2 discretetime phase-locked loops containing feedback delays," IEEE Trans. on Cir. and Sys. II: Express Briefs, vol. 56, no. 12, pp. 886–890, Dec. 2009.
[9] A. G. Yepes, F. D. Freijedo, J. Doval-Gandoy, O. Lopez, J. Malvar, and P. FernandezComesana, "Effects of discretization methods on the performance of resonant controllers," IEEE Trans. on Power Electron., vol. 25, no. 7, pp. 1692–1712, Jul. 2010.
[10] K. Arun and K. Selvajyothi, "Variable sampling composite observer based frequency locked loop and its application in grid connected system," Advan. in Elec. and Comp. Eng., vol. 16, no. 2, pp. 33–42, May 2016.
[11] P. Lamo, F. Lopez, A. Pigazo, and F. J. Azcondo, "An efficient FPGA implementation of a quadrature signal-generation subsystem in SRF PLLs in single-phase PFCs," IEEE Trans. on Power Electron., vol. 32, no. 5, pp. 3959–3969, May 2017.
[12] C. Kaufmann, C. C. Yez, and G. Pangalos, "Fast power system frequency estimation by shape class approximation for synthetic inertia provision by battery energy storage systems," in IEEE Int. Symps. on Power Electron. for Distri. Gen. Sys. (PEDG), Sep. 2020, pp. 309–314.
[13] P. G. Bhat, D. R. Shetty, Jayasankar V N, and Vinatha U, "Design and FPGA implementation of dual self-tuning filter based controller for single phase shunt active filter," 2019 Inn. in Power and Advan. Comp. Tech. (i-PACT), Mar. 2019.
[14] H. Ahmed, S. Biricik, and M. Benbouzid, "Extended self-tuning filter-based synchronization technique for unbalanced and distorted grid," Int. Conf. on Smart Power Inter. Energy Sys. (SPIES), Sep. 2020, pp. 350–355.
[15] J. Shekel, "Instantaneous frequency," in Proc. IRE, vol. 41, 1953, p. 548.
[16] Voltage Characteristics of Electricity Supplied by Public Distribution Systems, Eur. Std. EN–50160, 2008.